

# CFD analysis of Post Combustion process and refractory melting in EAF due to liquid metal vaporisation.

## Modelling & Experiment

Anshuman Sinha <sup>1</sup>, Dinesh Nath, Sumanta Maji, Amarendra Kumar Singh\*.  
IIT Kanpur.

### Abstract

*What is the message you wish to convey?*

Post combustion in EAF has led to enhancement of energy efficiency. In the current project CFD based model of post combustion is implemented on ANSYS Fluent. The post combustion model is based on the conservation of mass, momentum, energy and species and accounts for the high temperature reactions. The input to the model are Decarburization rate in the furnace, Oxygen stream flow rate, position of oxygen nozzle, Reaction mechanism, Reaction kinetics. Mathematical modelling of reacting turbulent flows is a challenging task. Here, the chemical reactions, flow characteristics along with dynamically changing thermo-physical properties need to be attended all together.

The process in itself is a turbulent non-premixed combustion however we have tried modelling it with species transport model along with solving the energy equation. The results for temperature and flow fields are well in agreement with the previous works. And over and above this approach gives us a benefit to model the wall surface reaction which may give us the electrode consumption rate.

Steelmaking is an energy intensive process and many advancements have been done in order to optimise the cost of production of steel. One of those major advancements have been in the field of refractories. Several practices have been implemented in the past to select the refractory material and to ensure the refractory life of these furnaces. All these practices of refractory selection and design have studied the heat transfer phenomenon taking place inside the furnace along with the chemical reactivity of phases which are present inside the furnace.

While many aspects like radiation, conduction, convection etc have been observed and taken care of while designing refractory, the author proposes to add a different dimension towards the furnace design by including a vaporisation-condensation based heat-mass transfer of liquid metal to the surrounding refractory.

The various aspects were modelled and compared in order to predict the melting of refractory which was observed in experimental heat at the. \* The integrated Steel making & Research Laboratory, IIT Kanpur. And the subsequent methods for prevention of these refractory losses was suggested.

\* The integrated Steel making & Research Laboratory, IIT Kanpur.  
Western Labs 102,  
IIT Kanpur.

### Keywords

Steelmaking, Furnace, Cost, Selection & Design, Optimisation, Refractory melting, Refractory life, Productivity, Market, Metal vaporisation, condensation, Heat transfer mechanism.

### Tentative Title

CFD analysis of Post Combustion process and refractory melting in EAF due to liquid metal vaporisation.

## Conclusion Outline

Heat transfer phenomena,  
Species transport,  
Mass transfer phenomena,  
Refractory melting phenomena,  
Arcing process,  
Optimisation of productivity,  
Timeline of arcing,  
Discuss Scrap melting models.

The heat transfer phenomenon and the corresponding refractory melting phenomenon as discussed in the present work agrees well with the experimentation and it's corresponding mathematical model. The proposed metal vaporisation-condensation based mass transfer phenomenon leads to a new dimension towards heat transfer phenomenons and refractory design considerations of the furnace. The process of arcing can now be optimised, so as to balance between quickly melting the metal and refractory losses due to continuous prolonged arcing. Now a new pattern/ timeline of arcing may be set which would benefit the overall process. The present scrap melting models shall also include the discussed heat transfer phenomena in order to correctly predict the melting behaviour of the scarp.

## Core section Outline

### Mathematical:

[Anshuman Sinha]

Post combustion model  
Evaporation-Condensation model  
Multiphase fluid flow model  
Lagrangian particle model  
Refractory selection parameters

[Dinesh Nath]

Arcing model  
Refractory heating model  
Furnace design parameters  
Scrap melting model

### Experimental:

[Sumanta]

Physical setup  
Metal traces on refractory  
Scrap concentration  
Refractory initial composition  
Furnace Temperature measurements  
Images

## A. Post Combustion, Multiphase fluid flow model:

Post combustion in EAF has led to enhancement of energy efficiency. In the current project CFD based model of post combustion is implemented on ANSYS Fluent, and is in the process of getting integrated with other modules of EAF\_OPT.

The post combustion model is based on the conservation of mass, momentum, energy and species and accounts for the high temperature reactions. The input to the model are Decarburisation rate in the furnace, Oxygen stream flow rate, position of oxygen nozzle, Reaction mechanism , Reaction kinetics .

And the model provides the output as Furnace Temperature, Flue gas final composition, Velocity profile inside the furnace, Energy utilisation from enthalpy data.

### Geometry setup and mesh

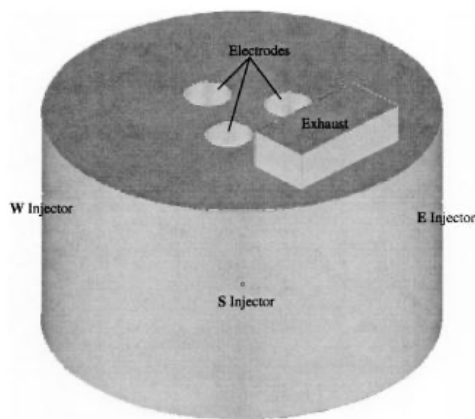


Fig. 1—Schematic of the EAF modeled.

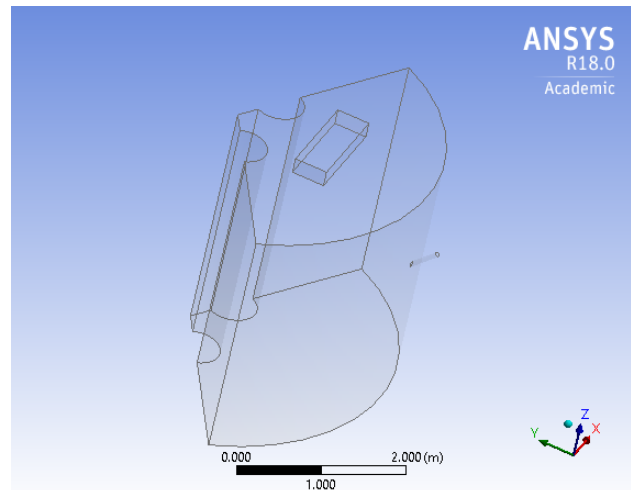


Fig 1: Setup geometry from Fruehan et al. (left), Simulation geometry (right)

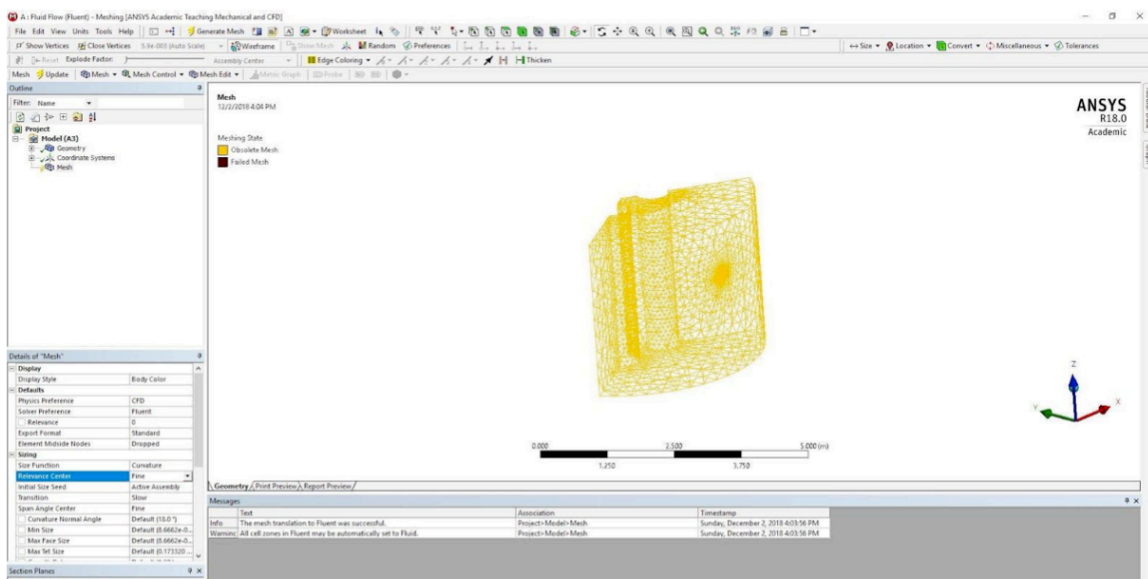


Fig 2: Simulation mesh generation through Ansys mesh generator

### CFD Three-Phase Flow Formulation

A three-dimensional transient mathematical model for argon gas stirred ladle which accounts for the steel, slag, and argon phases has been developed. A set of Navier–Stokes equations with incorporation of volume of fluid (VOF) function has been solved to investigate the dynamic behaviour of the three phases. The following set of transport equations<sup>[31,32]</sup> are solved.

Conservation of mass (continuity equation):

$$\frac{\partial \rho}{\partial t} + \nabla \cdot (\rho \vec{v}) = 0, \quad [1]$$

where  $\rho$  is the density of the mixture,  $t$  is time, and  $\vec{v}$  is the local velocity.

Conservation of momentum:

$$\frac{\partial}{\partial t}(\rho \vec{v}) + \nabla \cdot (\rho \vec{v} \vec{v}) = -\nabla p + \nabla \cdot [\mu_e (\nabla \vec{v} + \nabla \vec{v}^T)] + \rho \vec{g} \quad [2]$$

where  $p$  is the local pressure,  $\vec{g}$  is the acceleration due to gravity, and  $\mu_e$  is the effective viscosity. The effective viscosity is calculated as sum of dynamic and turbulent viscosities.

Turbulence: k- $\epsilon$  model

Standard k- $\epsilon$  model is used to capture the turbulence phenomenon. Following two transport equations of turbulent kinetic energy and its dissipation rate are solved to calculate the effective viscosity.

$$\frac{\partial(\rho k)}{\partial t} + \frac{\partial(\rho k u_i)}{\partial x_i} = \frac{\partial}{\partial x_i} \left[ \left( \mu + \frac{\mu_t}{\sigma_k} \right) \frac{\partial k}{\partial x_i} \right] + G_k - \rho \epsilon, \quad [3]$$

$$\begin{aligned} \frac{\partial(\rho \epsilon)}{\partial t} + \frac{\partial(\rho \epsilon u_i)}{\partial x_i} = & \frac{\partial}{\partial x_i} \left[ \left( \mu + \frac{\mu_t}{\sigma_\epsilon} \right) \frac{\partial \epsilon}{\partial x_i} \right] \\ & + C_{1\epsilon} \frac{\epsilon}{k} (G_k + C_{3\epsilon} G_b) - C_{2\epsilon} \rho \left( \frac{\epsilon^2}{k} \right) \end{aligned} \quad [4]$$

In Eqs. [3] and [4],  $k$  is the turbulent kinetic energy,  $\epsilon$  is the turbulent kinetic energy dissipation rate,  $x_i$  represents the spatial coordinates for different directions. The  $G_k$  and  $G_b$  terms represent the generation of

turbulent kinetic energy due to mean velocity gradient and the generation of turbulent kinetic energy due to buoyancy, respectively. These terms are calculated through Eqs. [5] and [6], respectively.

$$G_k = -\rho u_i u_j \frac{\partial u_i}{\partial x_j}, \quad [5]$$

$$G_b = -g_i (\mu_t / \rho Pr_t) \frac{\partial \rho}{\partial x_i} \quad [6]$$

$$\mu_t = \rho C_\mu \left( \frac{k^2}{\varepsilon} \right) \quad [7]$$

The turbulent viscosity is calculated by Eq. [7] using the  $k$  and  $\varepsilon$  from Eqs. [3] and [4] respectively. In these equations many constants are used whose values are as follows:  $C_{1e} = 1.44$ ,  $C_{2e} = 1.92$ ,  $C_1 = 1.44$ ,  $r_k = 1.0$ ,  $C_{3e} = 1.0$ , and  $r_e = 1.3$ .<sup>[31,32]</sup> Finally,

Volume of Fluid (VOF) model

$$\frac{\partial \alpha_q}{\partial t} + (\vec{v} \cdot \nabla) \alpha_q = 0, \quad [8]$$

$$\alpha_g + \alpha_l + \alpha_s = 1, \quad [9]$$

$$\rho = \alpha_g \rho_g + \alpha_l \rho_l + \alpha_s \rho_s, \quad [10]$$

where  $\alpha$  and  $\rho$  are volume fraction and density of the each phase, respectively, in a cell where  $q$  can have

value of  $g$ ,  $l$ , and  $s$  for argon, steel, and slag phases. The VOF formulation assumes that the various phases present in the system are not interpenetrating. Therefore, each phase in a cell is represented by its volume fraction. Volume fractions are derived by solving the continuity equation for each phase given in Eqs. [8] and [9]. The density of the mixture is calculated by Eq. [10] and used in continuity, momentum, and turbulence modeling equations.

## Results:

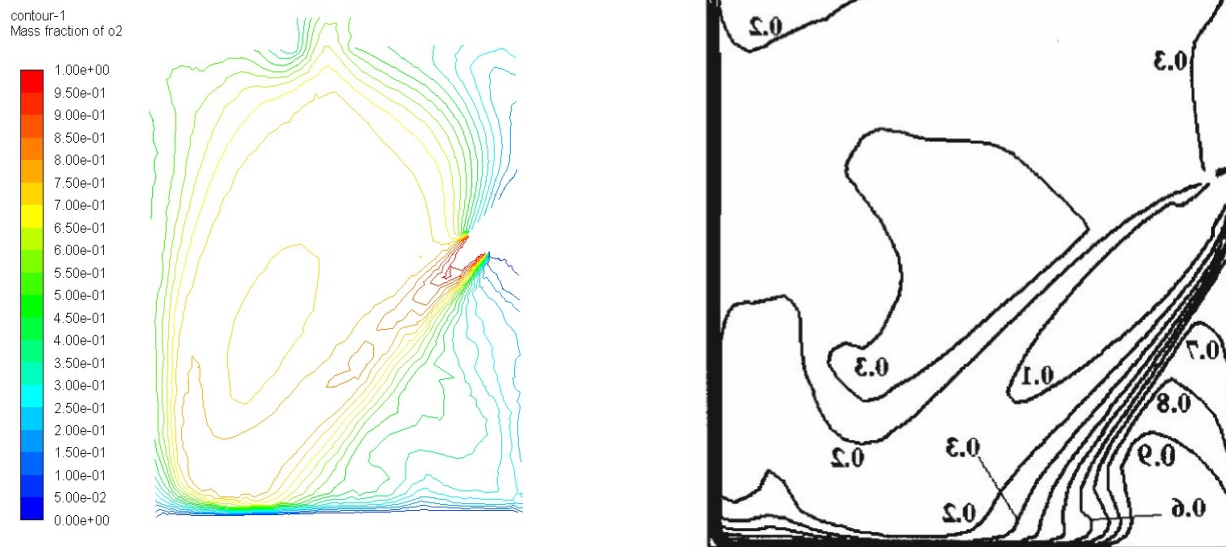


Fig 3: Combustion field on the plane intersecting the electrode of (a) Simulation (left) (c) Reference figure

Additionally it provides the rate of oxidation of the electrodes.

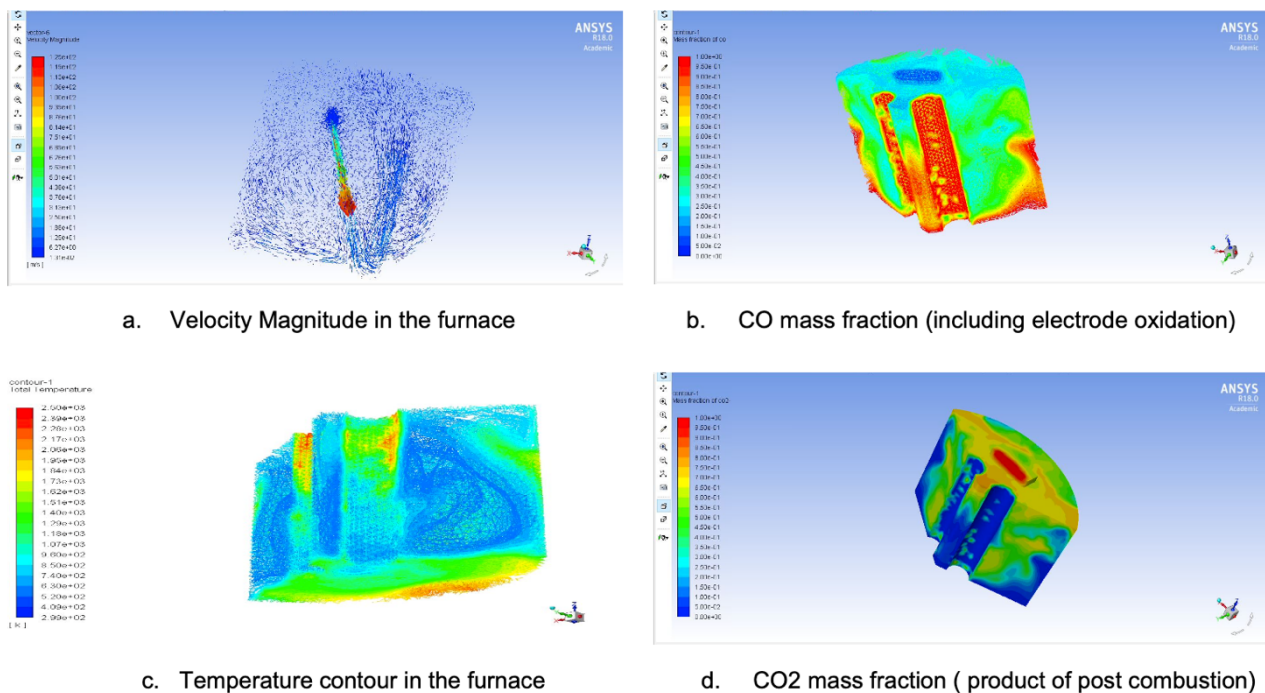


Fig 4: Various results of Post Combustion (a) velocity Magnitude in the furnace, (b) Carbon Mono-Oxide mass fraction, (c) Temperature contour in the furnace, (d) Carbon di-Oxide mass fraction.

Dealing with this gas phase system the species model is solved accompanied by the chemical reactions in both volumetric and wall surface regime. The turbulence mixing of species and corresponding chemical

reactions in the turbulent regime are modelled using the standard k- $\epsilon$  turbulence model and finite rate/ eddy dissipation respectively using the CFD software ANSYS-Fluent (Version 18)

The chemical reactions included in the model are for Post combustion reaction including the reverse reaction along with de-Post combustion reaction occurring at the walls of the electrode. The solution for temperature also includes the effect of radiation which accounts for the majority of the overall heat transfer.

The oxygen flow rate is restricted by the flame length which should be long enough that it does not intersect the bath directly. But since the fuel is in limited amount and is controlled by the bath chemistry and corresponding chemical reactions, hence we need to optimize the flow rate in order to combustion of the CO from the bath. For this several flow rates were simulated and an optimum flow rate of 0.32 m<sup>3</sup>/sec was found out to be most efficient for the combustion process.

The fuel (Carbon monoxide) entering the reactor at rate 2.5kg/s upon combustion produces an average temperature simulated is well within the adiabatic flame temperature as the PC is not ideal with stoichiometric amount of oxidizer ( $T_{avg} = 2420K$ ) and a poor recovery of the total heat produced is obtained mainly due to the flat bath condition (around 15% of the total heat produced).

[31] B. Li, H. Yin, C.Q. Zhou, and F. Tsukihashi: ISIJ Int., 2008, vol. 48 (12), pp. 1704–11.

[32] H. Liu, Z. Qi, and M. Xu: Steel Res. Int., 2011, vol. 82 (4), pp. 440–58.

[40] A. Ghosh: Secondary Steelmaking, Principles and Applications, CRC Press LLC, New York, 2001

## **B. Evaporation and condensation model:**

### **MODELING OF THE EVAPORATION AND CONDENSATION PHASE-CHANGE PROBLEMS WITH FLUENT**

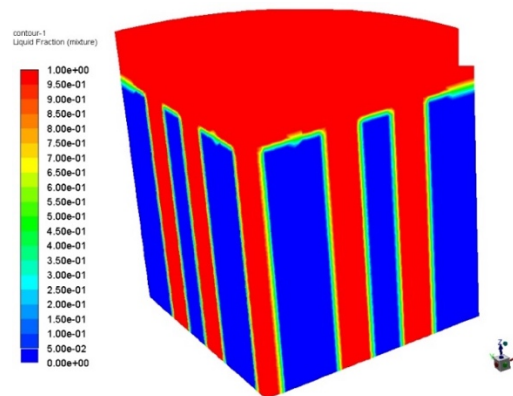


Fig 5: Liquid fraction profile for melting of porous material

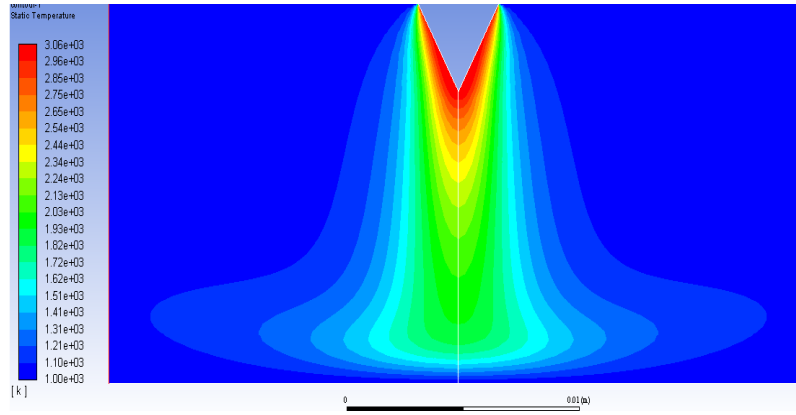


Fig 6: Temperature distribution during arcing

Evaporation is the process of turning a liquid, at its saturation temperature, into vapor by applying heat. The process reverse to evaporation is condensation, where vapor turns into liquid due to the removal of heat.

Because there is no universal model for mass transfer, ANSYS FLUENT provides a UDF that you can use to input models for different types of mass transfer, e.g. evaporation, condensation, boiling, etc. Note that when using this UDF, ANSYS FLUENT will automatically add the source contribution to all relevant momentum and scalar equations. This contribution is based on the assumption that the mass "created" or "destroyed" will have the same momentum and energy of the phase from which it was created or destroyed. If you would like to input your source terms directly into momentum, energy, or scalar equations, then the appropriate path is to use UDFs for user-defined sources for all equations, rather than the UDF for mass transfer.

Many methods have been proposed to simulate the vapor/liquid phase-change problems, such as the volume-of-fluid (VOF) method [1–3] and the level set (LS) method.

The VOF method has an inherent mass conservation property, more easily capturing interface with heat transfer of phase change [7]. The feature of mass conservation is particularly important when solving phase-change problems [8]. Therefore, it is a good choice to use the VOF method. At present, the VOF method has been employed in the FLUENT code to solve two-phase flows. However, the default VOF method cannot simulate heat and mass transfer through the phase interface. To overcome this short coming, the phase-change model needs to be added to the source terms in the governing equations using user-defined functions (UDFs).

There are many different kinds of phase-change models in references. The use of empirical expressions to quantify the interfacial heat and mass transfer appears to be a common way to model the phase-change phenomena [9, 10]. The approach is indeed valuable for certain simple geometries. However, its application is limited for any other geometry [11].

The phase-change model proposed by Lee [12] has been most widely used. The mass transfers are given by the following equations:

$$\dot{m}_v = -\dot{m}_l = r\alpha_l\rho_l \frac{T - T_{\text{sat}}}{T_{\text{sat}}} \quad T > T_{\text{sat}} \text{ (evaporation process)} \quad (1)$$



$$\dot{m}_l = -\dot{m}_v = r\alpha_v\rho_v \frac{T_{\text{sat}} - T}{T_{\text{sat}}} \quad T < T_{\text{sat}} \text{ (condensation process)} \quad (2)$$

where  $r$  denotes the mass transfer intensity factor with unit  $\text{s}^{-1}$ . The value of  $r$  is recommended to be such as to maintain the interfacial temperature reasonably close to the saturation temperature, and to avoid divergence issues. As an empirical coefficient,  $r$  is given different values for different problems. In the numerical studies of Wu et al. [13], De Schepper et al. [14], and Alizadehdakhl et al. [15],  $r$  was set as  $0.1 \text{ s}^{-1}$  in order to numerically maintain the interface temperature close to the saturation temperature. However,  $r$  was specified at a different value,  $100 \text{ s}^{-1}$ , in [16] and [17].

To avoid the limitation of empirical expressions or empirical coefficients, it is essential to develop a purely theoretical and validated formulation that explicitly solves phase-change problems. Fourier's law, as a theoretical formulation, can be applied to estimate the interfacial heat flux jump and determine the corresponding mass transfer flux based on the latent heat. The interfacial heat flux jump and mass transfer flux can be calculated by the following expressions:

$$\|\vec{q}_I\| = \left[ \left( -\lambda_l \frac{\partial T}{\partial n} \Big|_l \right) - \left( -\lambda_v \frac{\partial T}{\partial n} \Big|_v \right) \right] \vec{n} \quad (3)$$

$$\dot{m}_l = -\dot{m}_v = \frac{(\|\vec{q}_I\| \cdot \vec{n}) A_{I,C}}{h_{fg} V_C} \quad (4)$$

where  $\vec{n}$  is the interfacial unit normal vector and points toward the liquid phase.  $A_{I,C}$  and  $V_C$  denote, respectively, the interface area in a grid cell and the corresponding grid cell volume.

According to Eqs. (3) and (4), many authors have developed their own program codes to simulate phase-change problems, such as Welch and Wilson [7] and Guo et al. [18]. The key point of these models is how to accurately calculate the heat fluxes on both sides of the interface. These models can simulate the evaporation and condensation problems accurately. However, the implementation process is very complicated, limiting the extension of these models to the FLUENT code.

$$\dot{m}_v = -\dot{m}_l = \frac{(\alpha_v \lambda_v + \alpha_l \lambda_l)(\nabla \alpha_l \cdot \nabla T)}{h_{fg}} \quad (5)$$

In [11], [19], and [20], the following phase-change model was derived according to Eqs. (3) and (4):

which is easy to implement in the FLUENT code. However, this model has some shortcomings. For example, the bubble growth rate is not relevant to the vapour thermal conductivity  $k^V$  in the growing process of a saturated bubble in superheated liquid. However, Eq. (5) contains the information of  $k^V$ , not matching the actual physical phenomena.

To overcome the shortcomings mentioned above, a phase-change model [21] was proposed by the present authors in 2012 as follows:

$$\dot{m}_v = -\dot{m}_l = \frac{2\lambda_l(\nabla\alpha_l \cdot \nabla T)}{h_{fg}} \quad (6)$$

As we know, the mass transfer appears at the phase interface. However, the interfacial mass transfer fluxes calculated by Eqs. (5) and (6) are distributed in a finite-thickness region near the interface, reducing the calculation accuracy.

In this article, to further improve the accuracy, a new phase-change model is built based on the volume-of-fluid (VOF) method in the FLUENT code. Finally, the accuracy of this new phase-change model is verified by two evaporation problems (a one-dimensional Stefan problem and a two-dimensional film boiling problem) and one condensation problem (single steam bubble condensation in sub cooled water).

### C. Refractory Melting:

Steelmaking is an energy intensive process and many advancements have been done in order to optimise the cost of production of steel. One of those major advancements have been in the field of refractories. As the refractory material which are placed along the walls of the furnace provide several uses like thermal insulation for the bath, [ add a few points ]. With all these benefits the refractory itself needs to be taken care off from the harsh bath conditions. Several practices have been implemented in the past to select the refractory material and to ensure the refractory life of these furnaces. All these practices of refractory selection and design have studied the heat transfer phenomenon taking place inside the furnace along with the chemical reactivity of phases which are present inside the furnace.

While many aspects like radiation, conduction, convection etc have been observed and taken care of while designing refractory, the author proposes to add a different dimension towards the furnace design by including a vaporisation-condensation based heat-mass transfer of liquid metal to the surrounding refractory.

The electric arc furnace uses heat energy in the form of plasma from the arc. This intense heat source provides sufficient heat to the metal in order to melt it. But when this heat source stays in contact with the liquid metal for a much longer duration then this may convert the liquid metal to it's vapour form. This metal vapour emanating from the vicinity of the arc carries a huge amount of heat in the form of latent heat of vaporisation.

*What are refractory?*

Refractories are the primary materials used by the steel industry in the internal linings of furnaces for making iron and steel, in vessels for holding and transporting metal and slag, in furnaces for heating steel before further processing, and in the flues or stacks through which hot gases are conducted.

### *Importance of refractory?*

Refractory is an important component of modern furnaces, Refractories are expensive, and any failure in the refractories results in a great loss of production time, equipment, and sometimes the product itself.

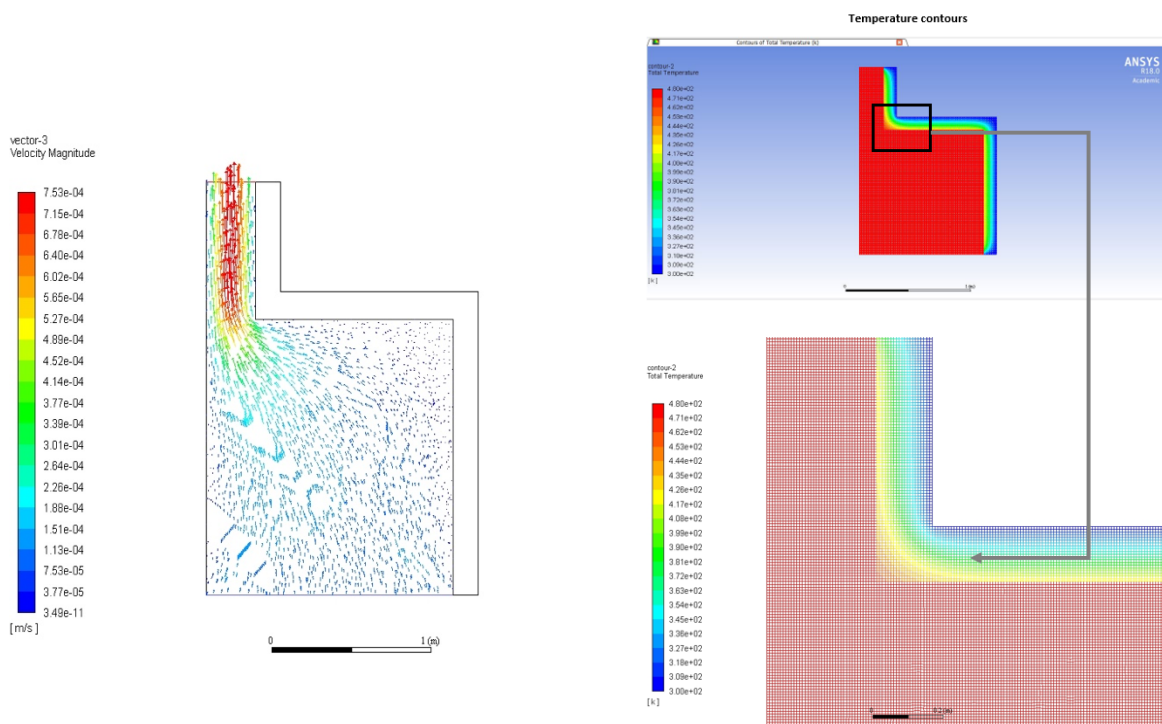


Fig 7: Refractory simulation for evaporated metal flow and temperature profile.

Physical Setup and Boundary Conditions

Outline of Results Discussions & Closure

## **D. Experimental:**

Setup and explanation of working principle.



Fig 8: Setup of experimental 50kg EAF